Nebulin regulates actin filament lengths by a stabilization mechanism

Christopher T. Pappas,[1,2] Paul A. Krieg,[1,2] and Carol C. Gregorio[1,2]

[1]Department of Cell Biology and Anatomy and [2]Sarver Molecular Cardiovascular Research Program, The University of Arizona, Tucson, AZ 85724

Efficient muscle contraction requires regulation of actin filament lengths. In one highly cited model, the giant protein nebulin has been proposed to function as a molecular ruler specifying filament lengths. We directly challenged this hypothesis by constructing a unique, small version of nebulin (mini-nebulin). When endogenous nebulin was replaced with mini-nebulin in skeletal myocytes, thin filaments extended beyond the end of mini-nebulin, an observation which is inconsistent with a strict ruler function. However, under conditions that promote actin filament depolymerization, filaments associated with mini-nebulin were remarkably maintained at lengths either matching or longer than mini-nebulin. This indicates that mini-nebulin is able to stabilize portions of the filament it has no contact with. Knockdown of nebulin also resulted in more dynamic populations of thin filament components, whereas expression of mini-nebulin decreased the dynamics at both filament ends (i.e., recovered loss of endogenous nebulin). Thus, nebulin regulates thin filament architecture by a mechanism that includes stabilizing the filaments and preventing actin depolymerization.

Introduction

Actin is the most abundant protein in most, if not all, cell types, and the regulation of actin filament architecture is critical for proper cellular function. Striated muscle cells display one of the most extreme examples of actin filament organization found in all of nature. The basic contractile units of striated muscle cells (sarcomeres) are composed of overlapping arrays of myosin (thick) and actin (thin) filaments that form a nearly crystalline structure. The thick and thin filaments interact with and slide past one another to produce contraction. Efficient contraction requires proper regulation of thin filament lengths. How the cell is able to specify and maintain these precise lengths is unknown. For more than two decades, the giant protein nebulin (600–900 kD) has been proposed by numerous investigators to function as a molecular ruler that defines the lengths of the thin filaments. Nebulin possesses several properties consistent with a function as a thin filament molecular ruler (Horowits, 2006; for reviews see Trinick, 1994; McElhinny et al., 2003). First, it extends along the entire length of the thin filament with its C terminus anchored within the Z-disc (a complex, protein-rich structure that connects two adjacent sarcomeres) and its N terminus extending out toward the center of the sarcomere (Wright et al., 1993). Second, the length of nebulin, which can vary as the result of alternative splicing, correlates with thin filament lengths in different muscle types (Kruger et al., 1991; Labeit et al., 1991). Finally, the unique protein structure of nebulin allows it to bind all the major components of the thin filament. For example, human nebulin is composed of 185 tandem copies of an ~35-aa repeat, each of which is thought to bind a single actin monomer (Jin and Wang, 1991; Labeit et al., 1991; Pfuhl et al., 1994; Labeit and Kolmerer, 1995). The majority of the repeats (modules 9–162) are also arranged into 22 consecutive seven-module super-repeats that match the periodicity of and are thought to interact with the thin filament components tropomyosin and troponin (Labeit and Kolmerer, 1995; Wang et al., 1996). Furthermore, the N terminus of nebulin binds the pointed end actin filament capping protein tropomodulin1 (Tmod1), which is located near the center of the sarcomere, whereas the C terminus interacts with the barbed end capping protein CapZ, which is located within the Z-disc (McElhinny et al., 2001; Pappas et al., 2008). Capping proteins effectively inhibit actin polymerization and depolymerization at the filament ends and are essential for proper thin filament

Correspondence to Carol C. Gregorio: gregorio@email.arizona.edu

Abbreviations used in this paper: G-actin, globular actin; Lat A, latrunculin A; Tmod, tropomodulin.

© 2010 Pappas et al. This article is distributed under the terms of an Attribution–Noncommercial–Share Alike–No Mirror Sites license for the first six months after the publication date (see http://www.rupress.org/terms). After six months it is available under a Creative Commons License (Attribution–Noncommercial–Share Alike 3.0 Unported license, as described at http://creativecommons.org/licenses/by-nc-sa/3.0/).

The Rockefeller University Press $30.00
J. Cell Biol. Vol. 189 No. 5 859–870
www.jcb.org/cgi/doi/10.1083/jcb.201001043

assembly and length regulation (e.g., Caldwell et al., 1989; Weber et al., 1994; Gregorio et al., 1995; Schafer et al., 1995; Sussman et al., 1998; Littlefield et al., 2001; Mudry et al., 2003). Thus, nebulin could specify the length of the thin filament by binding a specific number of actin and tropomyosin/troponin molecules and then recruit capping proteins, which would restrict assembly to that defined length.

Recently, analysis of nebulin in vivo has revealed its critical role in maintaining proper skeletal muscle function. Nebulin-deficient mice die within 2 wk of birth because of muscle weakness (Bang et al., 2006; Witt et al., 2006). Similarly, mutations in human nebulin can cause the muscle disorder nemaline myopathy, which is also characterized by muscle weakness (Pelin et al., 1999; Sanoudou and Beggs, 2001; Lehtokari et al., 2006). Analysis of skeletal muscle from nebulin knockout mice and tissue from patients with one specific mutation in nebulin that results in nemaline myopathy revealed that both have shorter thin filaments (Bang et al., 2006; Witt et al., 2006; Ottenheijm et al., 2009). Identical results were also obtained after the knockdown of nebulin in primary cultures of chick skeletal myocytes (Pappas et al., 2008). These findings confirm that nebulin is essential for proper thin filament length regulation in skeletal muscle but do not provide a mechanism by which it functions.

Because of its giant size, susceptibility to proteolysis, and inability to purify it in its native state, progress in determining nebulin's function has been slow. However, recent data have implicated nebulin in a diverse range of cellular functions besides its proposed role as a thin filament molecular ruler. There is evidence that nebulin regulates contraction, both by optimizing the interaction of actin and myosin and by controlling calcium handling of the sarcoplasmic reticulum (Root and Wang, 1994, 2001; Ottenheijm et al., 2008; Bang et al., 2009; Chandra et al., 2009). Also, the C terminus of nebulin interacts with and appears to be regulated by the abundant intermediate filament protein desmin, suggesting that nebulin may be involved in maintaining the lateral alignment of myofibrils, a property essential for coordinated and efficient contractile activity (Bang et al., 2002; Conover et al., 2009; Tonino et al., 2010).

In this study, we set out to determine how nebulin regulates thin filament lengths by directly testing the molecular ruler hypothesis. Here, we show that replacement of full-length endogenous nebulin with a small synthetic nebulin (mini-nebulin) in chick skeletal myocytes did not result in the assembly of shorter thin filaments. Strikingly, however, after latrunculin A (Lat A)–induced actin depolymerization, the thin filaments that remained were never observed to depolymerize below the length of mini-nebulin, but either matched the length or were longer than mini-nebulin (e.g., full-length thin filaments). This indicates that mini-nebulin effectively stabilizes actin filaments of lengths equal to or greater than itself. Furthermore, endogenous nebulin also protected actin filaments from depolymerization and reduced the exchange of thin filament components. Mini-nebulin was able to reduce actin exchange at both ends of the filament, again indicating that it can effectively stabilize actin filaments that are longer than its own length. Mechanistically, these results indicate that nebulin regulates actin filament lengths by stabilizing the filaments and thereby preventing their depolymerization.

Results

Generation of a small synthetic nebulin molecule (mini-nebulin)

The definitive approach to determine if a molecule functions as a molecular ruler is to alter the size of the molecule and verify a corresponding change in the length of the structure it regulates. This has not been practical for nebulin because its large size and repetitive structure have precluded cloning of its full-length cDNA. To circumvent these problems, we designed a shorter version of human nebulin, mini-nebulin, and had its coding sequence synthesized de novo (Fig. 1 A). Mini-nebulin is ∼250 kD in size and includes the unique N- and C-terminal regions of nebulin plus 4 of nebulin's 22 super-repeats (SR 1–3 and 22), resulting in a shorter molecule that retains all identified unique binding sites (e.g., Tmod, CapZ, desmin, myopalladin, etc.; Bang et al., 2001, 2002; McElhinny et al., 2001; Pappas et al., 2008). Additionally, mini-nebulin contains a HA tag at its C terminus and a fluorescent tag (GFP or mCherry) at its N terminus. Mini-nebulin was introduced into cultured chick skeletal myocytes, and the cells were analyzed by immunofluorescence microscopy. Localization of the GFP tag on mini-nebulin marked two distinct bands on either side of the Z-disc, indicating that the N terminus of mini-nebulin extends away from the Z-disc, whereas an anti-HA antibody stained within the Z-disc, indicating that the C terminus is located within the Z-disc (Fig. 1 B, arrowheads and arrows, respectively). The calculated mean distance between the N termini of mini-nebulin molecules extending in opposite directions from the Z-disc was 0.45 ± 0.1 µm (n = 89), whereas the distance between the N termini of endogenous nebulin was ∼2 µm. Thus, full-length mini-nebulin is successfully transcribed and translated and uniformly assembles in the same orientation as endogenous nebulin but extends a shorter distance from the Z-disc. Because the sequence of mini-nebulin is based on that of human nebulin, siRNA targeted against chick nebulin transcripts should not affect its expression. To confirm this, we cotransfected mini-nebulin– and chick nebulin–specific siRNA into chick myocytes and analyzed the cell lysates by Western blotting. As expected, siRNA treatment reduced endogenous nebulin levels (∼700 kD) by >90%, whereas mini-nebulin levels (250 kD) remained unchanged (Fig. 1 C).

Because of the very different sizes of mini-nebulin, which extends a short distance from the Z-disc, and endogenous nebulin, which extends nearly to the center of the sarcomere, both proteins could be detected simultaneously with an anti–N-terminal nebulin antibody in control cells (Fig. 2 A, e). (Note that the fluorescent secondary antibody used for the nebulin staining [Texas red] was visualized in the same channel in which the mini-nebulin tag [mCherry] was detected. Thus, the mini-nebulin labeling is a combination of mCherry and Texas red signals.) Staining with the anti–N-terminal nebulin antibody also revealed that mini-nebulin was able to displace endogenous nebulin (Fig. 2 A, i, arrow). This displacement resulted in actin filaments that were more accessible to phalloidin staining and shorter (indicated by the presence of a distinct gap in phalloidin staining at the M-line that was not observed in the control myocytes; Fig. 2 A, j, arrow). The length of the actin filaments from

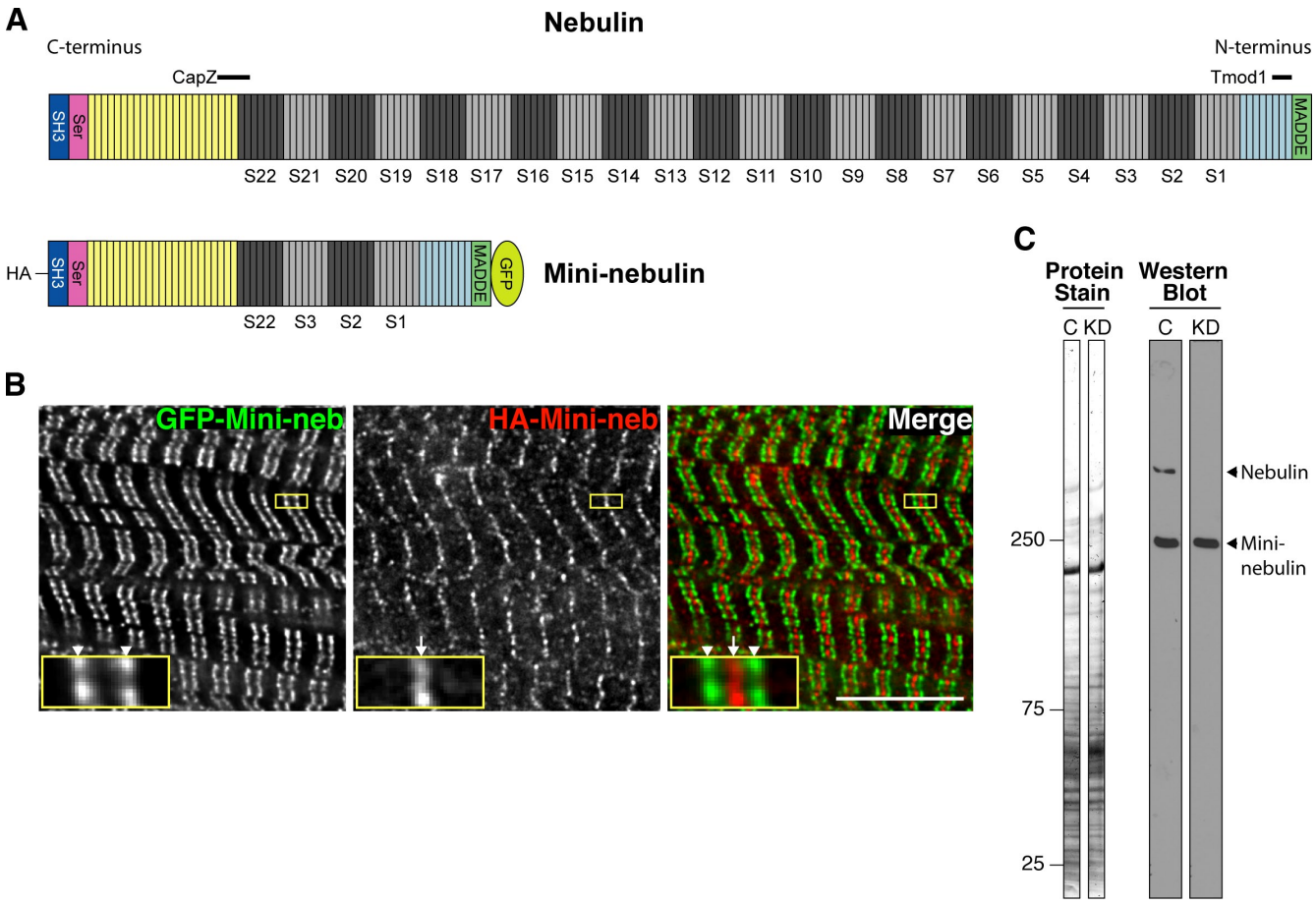

Figure 1. **A small synthetic version of nebulin (mini-nebulin) assembles in the same orientation as endogenous nebulin in chick skeletal myocytes.** (A) Schematic illustrating the structure of full-length human nebulin protein, which has 185 actin-binding modules of ~35 residues (small boxes) that are flanked by unique N- (MADDE) and C-terminal (serine rich and SH3) domains. The central repeats are further organized into seven-module super-repeats (SR 1–22), which bind troponins and tropomyosins. Binding sites of the capping proteins Tmod and CapZ are also noted. To construct a smaller version of nebulin (mini-nebulin), super-repeats 4–21 were removed, resulting in a molecule that is approximately one third of the size of endogenous nebulin. Mini-nebulin was tagged with GFP (or mCherry) at its N terminus and HA at its C terminus. (B) Chick skeletal myocytes transfected with GFP–mini-nebulin were costained with antibodies to GFP and HA. GFP, and thus the N terminus of mini-nebulin, was located on either side of the Z-disc (arrowheads), whereas HA displayed a single band within the Z-disc (arrows). This is the identical orientation that endogenous nebulin adopts. Boxes indicate the area that is enlarged in the insets. (C) Western blot analysis with an anti–C-terminal nebulin antibody revealed that chick skeletal myocytes produced full-length mini-nebulin protein whose expression is not affected by chicken-specific nebulin siRNA, unlike that of endogenous nebulin. Equivalent protein loading was verified by Ponceau S staining. Molecular mass is indicated in kilodaltons. C, control (scrambled siRNA–treated cells); KD, knockdown (nebulin-specific siRNA–treated cells). Bar, 10 µm.

pointed end to pointed end in these cells averaged 1.84 ± 0.13 µm (n = 57), which was ~15% shorter than the length obtained from control cells lacking mini-nebulin (2.16 ± 0.09 µm; n = 48; $P < 0.001$; Fig. 2 A, b). See Materials and methods for details on measurements. These results remarkably mimic alternations in actin architecture observed after the siRNA-mediated knockdown of nebulin (Fig. 2 B, b; Pappas et al., 2008). However, the knockdown of nebulin resulted in an ~24% reduction in actin filament lengths (1.65 ± 0.06 µm; n = 48; $P < 0.001$). These data suggest that mini-nebulin assembles on the actin filament in a manner similar to endogenous nebulin.

Mini-nebulin does not restrict thin filament lengths

To directly test the proposed ruler function of nebulin, mCherry–mini-nebulin was introduced into chick skeletal myocytes depleted of endogenous nebulin via nebulin-specific siRNA. In these myocytes, an N-terminal nebulin antibody stained bright bands flanking the Z-disc (corresponding to mini-nebulin) but did not stain near the center of the sarcomere (corresponding to endogenous nebulin; Fig. 2 B, e and i, arrows mark Z-discs). Strikingly, when cells expressing mini-nebulin were stained with fluorescently labeled phalloidin, actin filaments extending beyond the N-terminal end of mini-nebulin were clearly visible (Fig. 2 B, j and l, arrowheads). Extension of the thin filaments beyond the end of mini-nebulin was confirmed with an anti–cardiac actin antibody (unpublished data). The mean length of the actin filaments from pointed end to pointed end was 1.68 ± 0.08 µm (n = 53), which was not significantly different than in the knockdown alone. To determine if a population of actin filaments matching the length of mini-nebulin was obscured by longer actin filaments, myocytes expressing mini-nebulin were also stained for Tmod1, which marks the pointed ends of the actin filaments. Tmod1 staining was present in the

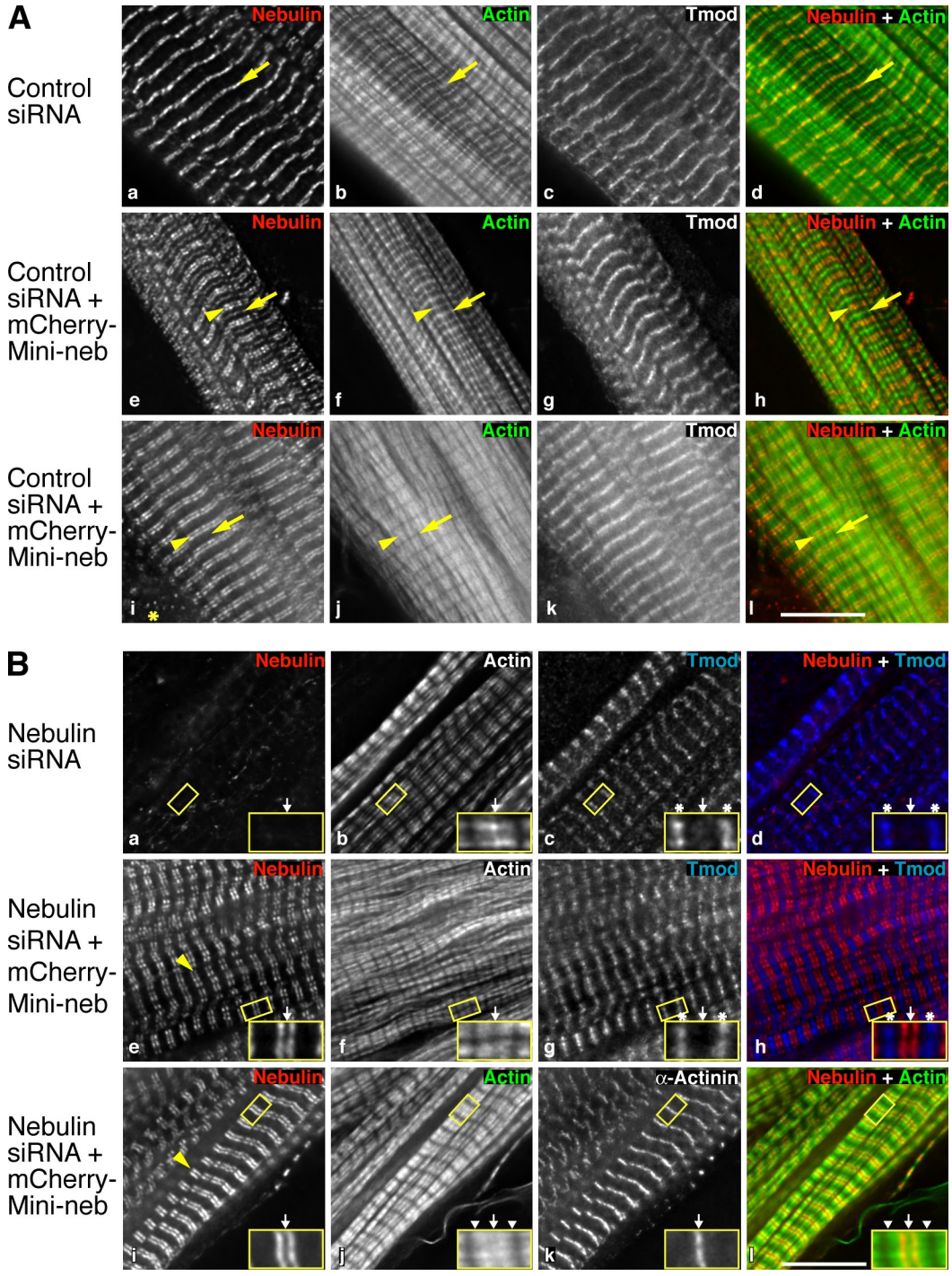

Figure 2. **Mini-nebulin can displace endogenous nebulin and does not restrict actin filament lengths or Tmod1 localization.** (A) Chick skeletal myocytes cotransfected with control siRNA alone or control siRNA plus mCherry–mini-nebulin were triple stained with fluorescently conjugated phalloidin (which labels F-actin; b, f, and j) and antibodies to N-terminal nebulin (a, e, and i) and Tmod1 (c, g, and k). The antinebulin antibody recognized both endogenous nebulin (arrows) and mini-nebulin (arrowheads). The top row (a–d) is a cell with no detectable mini-nebulin. The middle row (e–h) is a cell with both assembled mini-nebulin and endogenous nebulin. The bottom row (i–l) depicts a cell with mini-nebulin but no detectable endogenous nebulin. An asterisk marks protein aggregates that were often present in cells expressing the highest levels of mini-nebulin. Note that the displacement of endogenous nebulin resulted in shorter actin filaments as well as phalloidin staining along the entire length of the actin filaments, similar to what is observed in nebulin siRNA–treated cells. (B) Chick skeletal myocytes cotransfected with nebulin siRNA alone or nebulin siRNA plus mCherry–mini-nebulin were triple stained with fluorescently conjugated phalloidin (b, f, and j) and antibodies to N-terminal nebulin (a, e, and i) and Tmod1 (c and g) or α-actinin (k). Both the pointed ends of the actin filaments (which extend well past; white arrowheads) and Tmod1 (asterisks) failed to colocalize with the N terminus of mini-nebulin. Arrows denote Z-discs, and yellow arrowheads indicate mini-nebulin. Boxes indicate the area that is enlarged in the insets. Bars, 10 µm.

center of the sarcomere, at the location of the ends of actin filaments which were significantly longer than mini-nebulin, but no Tmod1 staining was detected in the vicinity of the N terminus of mini-nebulin (Fig. 2 B, g and h, asterisks); this suggests an absence of actin filaments that match the length of mini-nebulin. These data also suggest that despite the presence of a Tmod1-binding site, mini-nebulin is unable to direct the assembly of Tmod1. This is consistent with a recent report that Tmod1 and the N terminus of nebulin do not colocalize in various rabbit skeletal muscles (Castillo et al., 2009). Together, these data reveal that under these experimental conditions, mini-nebulin is unable to restrict actin lengths.

Nebulin stabilizes actin filaments

In a previous study, we observed that phalloidin stained along the entire length of the thin filaments in myocytes with reduced nebulin levels (Pappas et al., 2008). However, with nebulin levels unaltered, phalloidin staining was restricted to the ends of the filaments (a phenomenon which had previously been reported; Ao and Lehrer, 1995; Zhukarev et al., 1997). These observations indicated that nebulin and phalloidin compete for the same binding site on the actin filament. Accordingly, mini-nebulin is also able to inhibit phalloidin binding to actin filaments. A clear doublet of decreased phalloidin staining around the Z-disc was evident in cells expressing mini-nebulin (Fig. 2 B, f and j). Because phalloidin is known to bind to and stabilize actin filaments in vitro by reducing the dissociation rate of actin monomers from the polymer (Coluccio and Tilney, 1984), we hypothesized that nebulin may function in a similar manner in skeletal muscle cells.

To test the hypothesis that nebulin stabilizes actin filaments, we treated chick skeletal myocytes that had reduced levels of nebulin with the actin-depolymerizing agent Lat A. Cells depleted of nebulin displayed nearly complete depolymerization of actin filaments, as determined by staining with fluorescently labeled phalloidin. In many cells, only remnants of actin filaments within the Z-disc remained, marked by colocalization with α-actinin, an integral Z-disc protein (Fig. 3 A, e–h, arrows). This is not surprising because of the high number of actin-binding proteins within the Z-disc (for review see Clark et al., 2002). Conversely, actin filaments in myocytes treated with control siRNA were nearly unaffected by Lat A treatment (Fig. 3 A, a–d), a result which has been previously documented (Wang et al., 2005a). Because Lat A functions to depolymerize filaments by binding to monomeric actin (preventing its association with the polymer; Coué et al., 1987), the susceptibility of nebulin-deficient actin filaments to Lat A treatment suggests that nebulin significantly stabilizes actin–actin monomer associations within the filament.

Mini-nebulin stabilizes short and long actin filaments

To test whether mini-nebulin, like full-length endogenous nebulin, is capable of stabilizing actin filaments, we added Lat A to nebulin-depleted cells expressing mini-nebulin. Remarkably, in mini-nebulin–positive cells, actin filaments extended out from the Z-disc to a length that either matched or extended beyond the N terminus of mini-nebulin (Fig. 3 B, examples 1 and 2, respectively; arrows denote Z-discs and arrowheads mark the pointed ends of the actin filaments), whereas in cells lacking mini-nebulin, actin filaments were completely depolymerized or only observed within the Z-disc (Fig. 3 B, a–d). The locations of the pointed ends of the thin filaments (as a second marker for the length of the filaments) were then determined by staining for Tmod1 in cells extracted with a Triton X-100–containing buffer, which removes the cytosolic/soluble fraction of Tmod1, resulting in a clearer stain. In many cells, the localization of Tmod1 corresponded with the end of mini-nebulin, with no detectable Tmod1 near the M-line (Fig. 3 C, example 1; Zs mark Z-discs and arrowheads mark N-terminal mini-nebulin–matching Tmod1). In other cells, the distribution of Tmod1 appeared at both the end of mini-nebulin and near the M-line (Fig. 3 C, example 2; asterisks mark M-line Tmod1), indicating that full-length actin filaments as well as actin filaments at the length of mini-nebulin were present. Finally, a third population of cells had more intense Tmod1 staining near the M-line than at the end of mini-nebulin (Fig. 3 C, example 3). The percentage of the three distributions (i.e., examples 1–3) varied significantly (from ∼20 to 70%) from experiment to experiment, probably because of variations in cell density, maturation, efficiency of double transfections, and/or efficiency of depolymerization via Lat A. Notably, Tmod1 staining was not observed at lengths below that of mini-nebulin in any cell. However, in control cells treated with Lat A, Tmod1 staining was either punctate, with no recognizable assembly, or in distinct bands in close proximity to the Z-disc (likely marking the remnants of the depolymerized filaments; Fig. 3 C, top). To more clearly illustrate the location of actin and Tmod1 in relation to mini-nebulin after actin depolymerization, pixel intensity profiles of the staining along the longitudinal axis of the myofibrils were generated (Fig. 3 D). These data indicated that Lat A–induced actin depolymerization of full-length actin filaments was inhibited in the presence of mini-nebulin or progressed from the pointed ends of the filaments and stopped when reaching the N termini of mini-nebulin. These results indicate that mini-nebulin is capable of stabilizing thin filaments that are equal to or significantly longer than its own length. Therefore, nebulin functions to regulate thin filament architecture by preventing actin depolymerization.

Nebulin reduces the dynamics of thin filament components

If nebulin indeed stabilizes thin filaments, a reduction in nebulin levels would be predicted to increase the turnover of thin filament components. To test this, we used FRAP to determine the dynamics of thin filament proteins in chick skeletal myocytes. Myocytes were cotransfected with nebulin siRNA and GFP-actin. The incorporation of GFP-actin differed in the knockdown compared with the control. In control cells, GFP-actin assembled in a narrow band at the barbed ends (Z-disc; Fig. S1 b, arrow) and a wider band at the location of the pointed ends, in the center of the sarcomere (Fig. S1 b, arrowheads), with little incorporation along the length of the filaments. Conversely, in nebulin knockdown cells, GFP-actin was incorporated evenly throughout the filaments (Fig. S1 f). This observation indicates that, in the absence of nebulin, the central region of the actin

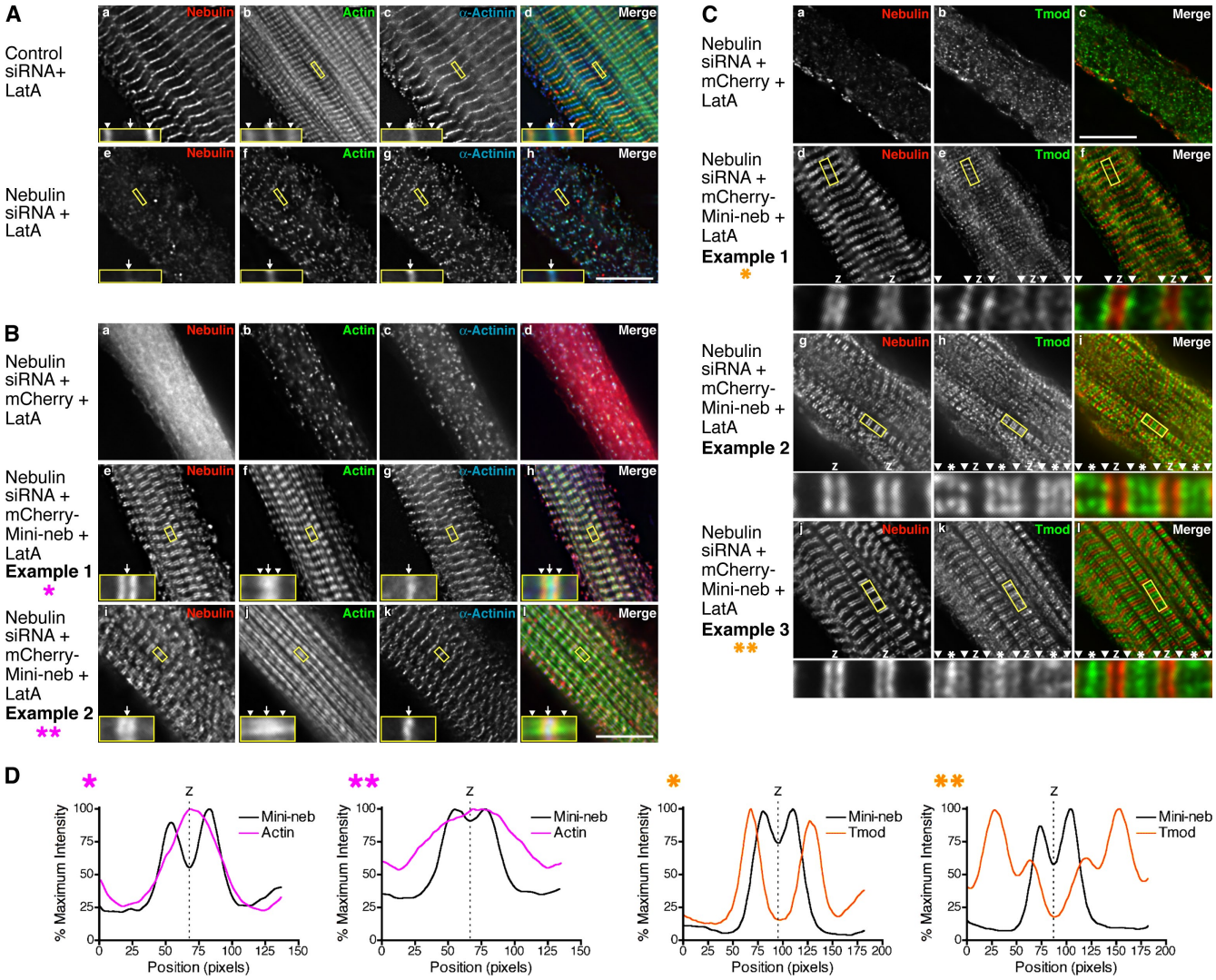

Figure 3. **Lat A treatment of chick skeletal myocytes with reduced nebulin levels results in actin filament depolymerization, whereas the introduction of mini-nebulin in these myocytes protects the filaments from depolymerization.** (A) Myocytes treated with Lat A for 9 h, 3 d after transfection of siRNA, were triple stained with fluorescently conjugated phalloidin (b and f) and antibodies to N-terminal nebulin (a and e) and α-actinin (c and g). The nebulin siRNA–treated cells (e–h) contained only remnants of F-actin at the Z-disc (arrows), whereas control siRNA–treated (a–d) cells were resistant to depolymerization, as indicated by the presence of full-length actin filaments (arrowheads mark the pointed ends). (B and C) Myocytes were cotransfected with nebulin siRNA and mCherry or mCherry–mini-nebulin and then treated with Lat A for 20–24 h, 5 d after transfection. (B) Cells were triple stained with fluorescently conjugated phalloidin (b, f, and j) and antibodies to N-terminal nebulin (a, e, and i) and α-actinin (c, g, and k). Cells expressing mini-nebulin had actin filaments that matched the length of mini-nebulin (example 1: e–h, arrowheads) or extended beyond the N-terminal end of mini-nebulin (example 2: i–l, arrowheads). Control cells again displayed actin filaments that were completely depolymerized or only observed within the Z-disc (a–d). Arrows denote the Z-discs. (C) Myocytes were also costained with an antibody to Tmod1 as a marker of actin filament pointed ends (b, e, h, and k). Example 1 (d–f) shows Tmod1 localization only in close proximity to the N termini of mini-nebulin (arrowheads). Example 2 (g–i) illustrates Tmod1 localization in close proximity to the N termini of mini-nebulin (arrowheads) and near the M-line (asterisks). Example 3 (j–l) shows more intense Tmod1 localization near the M-line (asterisks) than near the N termini of mini-nebulin (arrowheads). Zs denote the Z-discs. Note that cells were extracted in a Triton X-100–containing buffer before fixation to obtain a clearer Tmod1 stain; thus, most of the diffuse mCherry was removed with this treatment (top, nebulin). (A–C) Boxes indicate the area that is enlarged in the insets. (D) Pixel intensity plots of mini-nebulin and actin (top) or mini-nebulin and Tmod1 (bottom) from the examples illustrated in B and C (indicated by matching colored asterisks). The percentage of maximum intensity versus position of each pixel along the length of a myofibril is plotted. Each plot is centered on a single Z-disc and encompasses two half sarcomeres. Bars, 10 μm.

filament is more subject to actin turnover. This differential pattern of incorporation is nearly identical to that observed after phalloidin staining in both control and nebulin knockdown cells. Thus, the portion of the actin filament that is accessible to phalloidin (i.e., regions not associated with nebulin) also appears to be accessible to GFP-actin incorporation. Cells were photobleached in a defined area around the barbed (Z-disc) or pointed ends (center of the sarcomere) of the actin filaments and the recovery of fluorescence over time was monitored (Fig. 4 A, left; and Fig. S2). The mobile fractions from multiple experiments were determined from nonlinear regression curves fitted using a two-exponential association equation (Fig. 4 A, right). A significant increase in the mean slow mobile fraction was observed in cells with reduced levels of nebulin, whereas the mean fast mobile fraction remained unchanged. Thus, reducing the levels of nebulin increases the number of actin molecules that are able to exchange, which is consistent with the removal of a stabilizing mechanism.

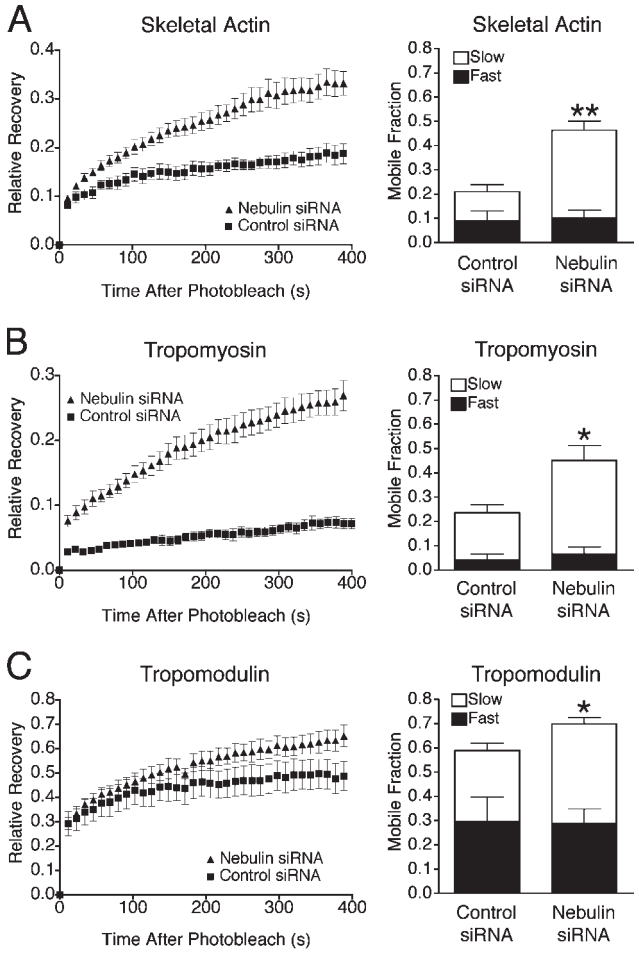

Figure 4. **The knockdown of nebulin in chick skeletal myocytes results in more dynamic thin filament components revealed by FRAP.** (A–C) Recovery after photobleaching of GFP–skeletal actin (A), GFP-tropomyosin (B), and GFP-Tmod1 (C) in control versus nebulin siRNA–treated chick skeletal myocytes. (left) Mean relative recovery from single representative experiments (n = 4–11 per treatment). (right) Mean slow and fast mobile fractions from two to three experiments (n = 8–17 cells per treatment). GFP–skeletal actin was bleached either at the Z-disc or M-line. Values are means ± SEMs. Asterisks indicate significant differences between treatments (*, $P < 0.05$; **, $P < 0.01$; Student's t test).

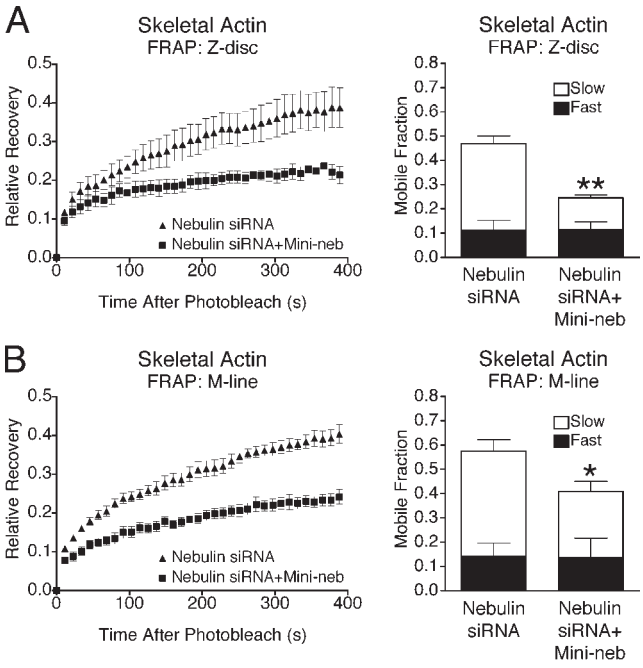

Figure 5. **Mini-nebulin recovers actin dynamics at both ends of the actin filament in cells with reduced levels of nebulin.** (A and B) Evaluation of the recovery after photobleaching of GFP–skeletal actin at the Z-disc (A) or M-line (B) in nebulin siRNA– versus nebulin siRNA plus mCherry–mini-nebulin–transfected chick skeletal myocytes. (left) Mean relative recovery curve from a representative experiment (Z: n = 4–5; M: n = 6–8 cells per treatment). (right) Mean slow and fast mobile fractions from two experiments (Z: n = 8–10; M: n = 12 cells per treatment). Values are means ± SEMs. Asterisks indicate significant differences between treatments (*, $P < 0.05$; **, $P < 0.01$; Student's t test).

To ascertain whether nebulin affects the dynamics of other thin filament components, the recoveries of GFP-tropomyosin and GFP-Tmod1 after photobleaching were also analyzed. Similar to the results obtained with GFP-actin, the mean slow mobile fractions of recovery of both tropomyosin and Tmod1 significantly increased in cells with reduced nebulin (Fig. 4, B and C, respectively). The increase in the number of exchangeable tropomyosin and Tmod1 molecules could be directly caused by the loss of the nebulin or indirectly caused by the increase in actin dynamics.

To further establish that mini-nebulin is capable of stabilizing actin filaments, chick skeletal myocytes were cotransfected with mCherry–mini-nebulin, GFP-actin, and nebulin siRNA. GFP-actin around the Z-disc or M-line was bleached, and recovery of fluorescence was monitored. Remarkably, introduction of mini-nebulin rescued the increased actin dynamics observed at both the barbed (Fig. 5 A) and pointed ends (Fig. 5 B) of the actin filaments seen when nebulin was depleted. In fact, the mean mobile fraction of barbed end actin associated with mini-nebulin was nearly identical to that observed in cells containing endogenous nebulin (Fig. 4 A, control siRNA). Therefore mini-nebulin decreases the number of actin molecules that exchange with the barbed and pointed ends of the thin filament, which is consistent with the addition of an actin stabilizer. Furthermore, these results support the Lat A experimental data, indicating that mini-nebulin can stabilize actin filaments without matching their lengths.

Discussion

In this study, we used a combination of tools to manipulate the architecture of actin filaments in skeletal muscle to determine how the giant molecule nebulin contributes to actin filament length regulation. Skeletal myocytes in culture were ideal for this study because we were able to significantly reduce endogenous levels of nebulin via siRNA, introduce a unique, small recombinant nebulin molecule (mini-nebulin), and chemically depolymerize the actin filaments. This combination of approaches could not be accomplished in intact animal models. Importantly, the sarcomeric alterations observed after the knockdown of nebulin in chick skeletal myocytes in culture match those observed after the knockout of nebulin in mice. Namely, both have shorter thin filaments, the presence of nemaline bodies, and wide, misaligned Z-discs (Bang et al., 2006; Witt et al., 2006; Pappas et al., 2008; unpublished data). Our data show that nebulin is not sufficient to function as a strict molecular ruler

(i.e., one in which the length of nebulin matches the length of the actin filaments) for specification of thin filament lengths because mini-nebulin was unable to restrict the growth of actin filaments or localize Tmod1. Instead, our data demonstrate that nebulin regulates thin filament lengths by decreasing actin depolymerization and thereby stabilizing the filaments.

Treatment of mature skeletal myocytes with the actin monomer–sequestering drug Lat A had remarkably little effect on actin filament architecture, indicating that the dissociation rate of actin monomers from the polymer was very low. However, after the removal of nebulin, actin filaments depolymerized upon Lat A treatment, demonstrating that the dissociation rate of actin monomers from the polymer filament had considerably increased. Additionally, using FRAP, we showed that nebulin reduces the dynamic exchange of actin, tropomyosin, and Tmod1 in the thin filaments. Because nebulin contains an unparalleled number of tandem actin-binding domains (~200), which have the potential to make numerous molecular contacts with the actin filament, it likely directly stabilizes the filament. However, because nebulin also binds to tropomyosin and tropomyosin itself has been shown to stabilize actin filaments (Broschat, 1990; Wang et al., 1996; Cooper, 2002), we predict that these two molecules act synergistically to produce mature filaments that are highly resistant to depolymerization. Finally, nebulin could also protect the actin filament from depolymerization factors such as DNaseI and ADF (actin-depolymerizing factor)/cofilin or severing by gelsolin, which has been shown to be an attribute of tropomyosin (Hitchcock et al., 1976; Bernstein and Bamburg, 1982; Fattoum et al., 1983; Ono and Ono, 2002).

We also showed that the length of nebulin determined the extent to which the actin filament was stabilized. When we replaced endogenous nebulin with mini-nebulin, only the portion of the thin filament not associated with mini-nebulin was susceptible to depolymerization because actin filaments shorter than mini-nebulin were not observed (both by phalloidin and Tmod1 staining). Surprisingly, mini-nebulin also transmitted stability to the entire actin filament, as indicated by its increased resistance to Lat A depolymerization, and decreased actin dynamics at both ends of the filament.

Our results support a model of thin filament length regulation in which nebulin dictates the minimal length at which the thin filament is stabilized and permits the filament to elongate to its final physiological length (Bang et al., 2006; Gokhin et al., 2009; for review see Littlefield and Fowler, 2008). Our data are also consistent with previous studies that demonstrated (a) via immunofluorescence microscopy that thin filaments extend past the N terminus of nebulin (Castillo et al., 2009), (b) that a two-module nebulin fragment is able to prevent actin depolymerization in vitro (Chen et al., 1993), and (c) that fluorescently labeled actin was more stable in myofibrils that had a mature staining pattern of nebulin (Nwe et al., 1999). Furthermore, studies of nebulin knockout mice have revealed that sarcomere structure and function progressively worsen with age and contractile activity (Bang et al., 2006; Witt et al., 2006; Chandra et al., 2009; Gokhin et al., 2009; Tonino et al., 2010), which could be the result of some level of thin filament depolymerization caused by a lack of nebulin-induced actin filament stability. As far as we know, our study provides the only direct evidence to date that nebulin stabilizes actin directly in cells and that this stability contributes to proper length maintenance.

We cannot rule out the possibility that because of its small size (one third of the size of endogenous nebulin), the ruler activity of mini-nebulin was rendered ineffective by the large amount of globular actin (G-actin) present when the thin filaments are that short. Nevertheless, the fact that mini-nebulin can influence the stability of portions of the actin filament with which it is not in immediate contact is also inconsistent with the classical model of a molecular ruler. Further evidence contradicting a strict ruler function of nebulin is its absence in most invertebrate skeletal muscles, which have regulated actin filament lengths. In fact, many invertebrates have extraordinarily long sarcomeres (e.g., 10 µm in the tarsonemid mite; Aronson, 1961); consequently, if nebulin were present, it would have to be approximately five times the length of vertebrate nebulin to function as a ruler, which seems unlikely. Thus, although nebulin may not function as an indispensable molecular ruler, we would predict, based on our data, that it provides a higher-order stabilization mechanism in vertebrates that is not required in lower organisms.

How can a change in actin filament stability translate to a change in thin filament lengths? An increase in actin dissociation caused by the loss of a stabilizer (e.g., nebulin) would likely increase the critical concentration of G-actin required for polymerization. Furthermore, Tmod has a much higher affinity for the pointed ends of actin filaments that are associated with tropomyosin (Weber et al., 1994). Therefore, more dynamic tropomyosin (caused by the loss of nebulin) would be predicted to result in more dynamic Tmod, with a lower affinity for the pointed end of the actin filament (which is consistent with our FRAP data). Less efficient Tmod capping (i.e., in the absence of tropomyosin) has been proposed to result in an increase in the critical concentration of actin in vitro (Weber et al., 1999). Therefore, this combined increase in the concentration of G-actin required for polymerization could result in a cell state in which the steady-state of exchange between G-actin and the filament is reached at a shorter mean filament length; this could explain the shorter thin filaments observed in nebulin knockout and knockdown models (Bang et al., 2006; Witt et al., 2006; Pappas et al., 2008).

How can nebulin confer stability to portions of the actin filament it does not associate with? One possible mechanism is that by stabilizing the Z-disc/I-band portion of the thin filament, nebulin may alter the structure of any individual or synergistic group of thin filament–associated proteins that may confer stability to the whole filament (e.g., titin and tropomyosin). Tropomyosin is an especially good candidate because it binds along the entire thin filament and is stabilized by nebulin. Clearly, extensive structural studies of thin filaments with and without nebulin are warranted in the future.

Our data demonstrate the ability of nebulin to inhibit the depolymerization of the actin filament but do not provide evidence that nebulin plays a role in regulating actin filament polymerization. Therefore, other factors such as Tmod may be involved in restricting the growth of actin filaments (Castillo et al., 2009; for review see Littlefield and Fowler, 2008). Alternatively, when actin filaments reach their final lengths, the cell may

be in a state that does not favor actin polymerization, and full-length actin filaments are maintained by the protection afforded by nebulin and tropomyosin. In support of this hypothesis, the concentration of G-actin is considerably lower in adult compared with embryonic chicken skeletal muscle (Shimizu and Obinata, 1986). In any case, it is clear from our present and previous studies as well as work from many other laboratories (for reviews see Littlefield and Fowler, 1998, 2008) that regulation of thin filament architecture requires the coordinated activity of many molecules/mechanisms.

Interestingly, Wang et al. (2007) reported that the dynamics of tropomyosin decrease as premyofibrils develop into mature myofibrils in skeletal myocytes. This is consistent with our data because nebulin is not found in its mature conformation in premyofibrils (Wang et al., 2007). In addition, tropomyosin is more dynamic in mature cardiac myocytes, which contain only minor amounts of nebulin, than in mature skeletal myocytes, in which nebulin is highly expressed (Wang et al., 2008).

The N terminus of nebulin associates with the pointed end of the actin filament near the center of the sarcomere, whereas the C terminus is located at the barbed end of the filament within the Z-disc (Wright et al., 1993). Previous studies have shown that only C-terminal fragments of nebulin associate with the thin filament when expressed in myocytes in culture, suggesting that the Z-disc portion of nebulin is necessary for its assembly (Ojima et al., 2000; Panaviene et al., 2007). Mini-nebulin, which we constructed with the complete unique N and C termini of nebulin (i.e., only the central region of nebulin was removed), assembled with its C-terminal end within Z-disc and N-terminal region extending out from the Z-disc. This observation indicates that the C terminus of nebulin directs its assembly and supports a model in which the C terminus of nebulin first associates with the Z-disc, and then the rest of the molecule assembles (zippers) along the thin filament (Chen et al., 1993). Because of the number of actin-binding repeats present within its structure, one molecule of mini-nebulin, if linear, would be predicted to extend ∼325 nm along the actin filament. Therefore, two molecules of mini-nebulin extending in opposite directions from the center of the Z-disc would measure ∼650 nm from end to end. However, the measured distance from end to end was 450 nm. This suggests that molecules of nebulin extensively overlap within the Z-disc, with the last super-repeat (22) located at the edge of the Z-disc. This result is consistent with a previous model of the molecular layout of nebulin within the Z-disc, which was based on the identification of binding sites of integral Z-disc proteins within nebulin (Pappas et al., 2008).

Understanding how nebulin functions is of particular importance because mutations in nebulin are the most common cause of the human muscle disorder nemaline myopathy (Pelin et al., 1999; Lehtokari et al., 2006). Nemaline myopathy is characterized by muscle weakness usually in the upper body, and its severity can vary from mild, with late onset and slow progression, to severe, with neonatal lethality caused by respiratory problems (Sanoudou and Beggs, 2001). A hallmark of the disease is the presence of rodlike nemaline bodies in the muscle fibers that are composed of aberrantly arranged Z-disc and thin filament (I-band) proteins. Notably, a recent study has directly linked a specific human mutation in nebulin, which results in nemaline myopathy, to improper (shorter) actin filament length regulation (Ottenheijm et al., 2009). Regulation of actin filaments lengths by nebulin also appears to be linked to certain desmin-related myopathies. Desmin is an abundant intermediate filament protein that localizes to the periphery of the Z-disc, where it interacts with C-terminal nebulin, and may function to laterally align adjacent myofibrils (Granger and Lazarides, 1979; Milner et al., 1996; Li et al., 1997; Bang et al., 2002; Tonino et al., 2010). Desmin-related myopathies result in skeletal muscle weakness, which is also often accompanied by cardiomyopathy (Goldfarb et al., 2004). At the cellular level, the disease is characterized by the presence of cytoplasmic protein aggregates that contain desmin. One specific mutation of desmin, which causes desmin-related myopathy, is located within the nebulin-binding domain. Introduction of desmin with this mutation into myocytes in culture leads to reduced nebulin assembly and unregulated actin filament lengths, which is consistent with defects observed in the human disease (Conover et al., 2009). Therefore, our study, which describes how nebulin regulates actin filament length, adds to a more complete understanding of these disease processes.

Nebulin regulation of actin filament length is likely not restricted to skeletal muscle because nebulin is expressed in a variety of other tissues that exhibit defined actin lengths, including the heart, kidney, eye, otic canal, and liver (Kazmierski et al., 2003; Bang et al., 2006). Finally, our results suggest that other proteins with multiple tandem actin-binding sites will have the potential to regulate actin filament architecture by a stabilization mechanism.

Materials and methods

Cell culture and siRNA treatment

Primary cultures of chick skeletal myocytes were prepared as described previously (Nawrotzki et al., 1995) with minor modifications. In brief, breast muscle was dissected from three to five 11-d-old chicken embryos, pooled, minced with scissors, and suspended in a 0.05% trypsin-EDTA solution (Cellgro). Cells were dissociated by gentle pipetting. The activity of trypsin was then quenched by adding growth medium (12.5% horse serum [HyClone], 12.5% chicken embryo extract, and 5 mM L-glutamine [Cellgro] in MEM [Cellgro]). The cell suspension was then centrifuged, resuspended in new growth medium, filtered with a 70-µm cell strainer (BD), and plated on uncoated culture dishes for 30 min, two times to remove fibroblasts. 9.5×10^5 unattached cells were plated on Matrigel (BD)-coated coverslips in a 35-mm dish. After 2 d, the growth medium was replaced with differentiation medium (12.5% horse serum, 2% chicken embryo extract, and 4.5 mM glutamine in MEM) that, if necessary, contained 1 µg/ml cytosine β-D-arabinofuranoside to prevent fibroblast proliferation. A nebulin-specific siRNA we previously designed and validated (Pappas et al., 2008) was purchased from Applied Biosystems (target cDNA sequence, 5′-GTAGCTGACTCTCCAATTA-3′). Random siRNA was also purchased (target cDNA sequence, 5′-CTCGACTAGAGTCTGTCTA-3′). Skeletal myocytes were transfected ∼13 h after plating with 50 nM of siRNA using the lipid-based reagent Effectene (QIAGEN) according to the manufacturer's instructions. For cotransfection experiments, GFP fusion expression constructs of 0.5–1 µg chicken Tmod1, chicken skeletal α-actin, and rat α-tropomyosin (gift from J.C. Perriard, Eidgenössische Technische Hochschule Zürich, Zürich, Switzerland; Helfman et al., 1999) were transfected ∼4 h after siRNA treatment to avoid toxicity problems. 3–5 d after transfection, the cells were incubated in relaxing buffer (150 mM KCl, 5 mM $MgCl_2$, 10 mM MOPS, pH 7.4, 1 mM EGTA, and 4 mM ATP) for 15 min and fixed with 2% paraformaldehyde in relaxing buffer for 15 min. When indicated, the cytosol of cells was extracted in cytoskeleton stabilization buffer (10 mM Pipes, pH 6.8, 100 mM KCl, 300 mM sucrose, 2.5 mM $MgCl_2$, and 0.5% Triton X-100 plus the protease inhibitors) before

fixation, as previously described (Gregorio and Fowler, 1995). For actin depolymerization experiments, a stock solution of Lat A (Invitrogen) was reconstituted to 20 mM in DMSO and then diluted to 2 mM with deionized H_2O and stored in single use aliquots at −80°C. 3–5 d after transfection, cells were treated for 9–20 h with 10 µM Lat A diluted in culture media. Cells in culture longer (i.e., 5 d) required longer Lat A treatments to obtain effective actin depolymerization, presumably because of their maturity. After treatment, to avoid repolymerization, cells were directly fixed with 2% paraformaldehyde in relaxing buffer.

Western blot analysis

Western blotting was performed as previously described (McElhinny et al., 2005) using polyclonal anti–C-terminal (1:1,500) and anti–N-terminal (1.4 µg/ml) nebulin antibodies and polyclonal anti-GFP (1:4,000) antibodies (Abcam). All antibodies recognized an ∼250-kD protein in lysates of chick skeletal myocytes transfected with mini-nebulin. Equivalent protein loading was verified by Ponceau S staining.

Immunofluorescence microscopy

Fixed cells were permeabilized in 0.2% Triton X-100/PBS, blocked with 2% BSA plus 1% normal donkey serum/PBS, and incubated for 1 h with primary antibodies diluted in PBS. The primary antibodies included a polyclonal anti–N-terminal nebulin (4.6 µg/ml), a monoclonal anti–α-actinin (1:10,000; Sigma-Aldrich), a polyclonal anti-GFP (1:300; Abcam; this antibody was used to enhance the signal of mini-nebulin so that more cells could be analyzed), a monoclonal anti–cardiac actin (1:10; American Research Products, Inc.), a monoclonal anti-Tmod1 (m95; 1:500), and a monoclonal Alexa Fluor 594–conjugated anti-HA antibody (5 µg/ml; Invitrogen). Staining the N terminus of nebulin often resulted in a single band of staining at the M-line, likely caused by contraction of the myofibrils. Alexa Fluor 488–conjugated phalloidin was used to stain F-actin (Invitrogen). The cells were then washed with PBS for 15 min and incubated with secondary antibodies/PBS for 30 min. The secondary antibodies, obtained from Invitrogen and Jackson ImmunoResearch Laboratories, Inc. included Alexa Fluor 488–conjugated goat anti–mouse IgG (1:1,000), Alexa Fluor 350–conjugated goat anti–mouse IgG (1:300), and Texas red–conjugated donkey anti–rabbit IgG (1:600). Coverslips were mounted onto slides with Aqua Poly/Mount (Polysciences, Inc.). The cells were analyzed, and images were captured using a Deltavision RT system (Applied Precision) with an inverted microscope (IX70; Olympus), a 100× NA 1.3 objective, and a charge-coupled device camera (CoolSNAP HQ; Photometrics) using SoftWoRx 3.5.1 software (Applied Precision). The images were then deconvolved using SoftWoRx and processed using Photoshop CS (Adobe). Over 200 cells were observed for each treatment/condition.

Actin filament and sarcomere lengths as well as the distance between the ends of mini-nebulin molecules extending in opposite directions from the Z-disc were ascertained from deconvolved images of cells stained with fluorescently conjugated phalloidin, anti–α-actinin, or anti–N-terminal nebulin antibodies, respectively, using ImageJ 1.42q software (National Institutes of Health). Pixel intensity profiles of the staining along the longitudinal axis of the myofibrils were generated, and the distance between mini-nebulin N termini or Z-disc to Z-disc was determined by measuring the distance from one peak of intensity to the next. Actin filament lengths were determined by measuring the distance from pointed end to pointed end, which represents actin filaments from two adjacent sarcomeres. If the pointed end could not be discerned (i.e., if there was no gap in phalloidin staining at the M-line), sarcomere lengths (Z-disc to Z-disc) were used as a measure of thin filament lengths (in this situation, this value is identical to M-line to M-line measurements). Note that this value represents the minimal possible thin filament length (i.e., we cannot determine if thin filament lengths are longer than sarcomere lengths). Values are means ± SD, and two-tailed, unpaired Student's *t* tests were used to determine the significance of differences (Excel; Microsoft).

FRAP

A Deltavision RT system with a 100× NA 1.3 objective and a CoolSNAP HQ charge-coupled device camera fitted with a 488-nm argon laser and environmental chamber was used for FRAP experiments. Cells were plated on glass-bottom dishes (MatTek), supplemented with 20 mM Hepes, and maintained at 37°C for the duration of the experiment. Three prebleach images were recorded, followed by photobleaching for 0.1 s at 100% power. To monitor recovery after photobleaching, images were captured at 10- or 20-s intervals for 400 s. Analysis of recovery was completed as described previously with minor modifications (Wang et al., 2005b). In brief, images were imported into ImageJ 1.37 software (National Institutes of Health), and mean intensities from bleached, nonbleached, and background regions were recorded. After background subtraction and correction for photobleaching caused by image acquisition, intensities were normalized so that prebleach intensity was set to 1 and postbleach intensity was set to 0. Mobile fractions were determined from nonlinear regression curves that were best fit using a two-exponential association equation ($R = M_{(fast)} \times (1 - \exp(-k_1 \times t)) + M_{(slow)} \times (1 - \exp(-k_2 \times t))$) with Prism 4 software (GraphPad Software, Inc.). R is the relative recovery at time t, and the total mobile fraction is the combination of $M_{(fast)}$ and $M_{(slow)}$. For the recovery experiments, control cells were treated with nebulin-specific siRNA alone or siRNA plus mCherry. 4–11 cells per treatment were analyzed in each experiment and two to three experiments were averaged. All values are means ± SEM, and two-tailed, unpaired Student's *t* tests were used to determine the significance of differences (Excel). After the FRAP experiments, the cells were fixed and stained to confirm knockdown of nebulin.

Mini-nebulin design, construction, and analysis

Mini-nebulin was designed using the coding sequence of human nebulin (available from GenBank/EMBL/DDBJ under accession number NM_004543) and the structural organization characterized by Labeit and Kolmerer (1995). To reduce the size of nebulin, 18 super-repeats were removed (SR 4–21), leaving the unique N and C termini and 4 super-repeats remaining (SR 1–3 and 22; Fig. 1 A). This resulted in a shorter molecule that retained all of its known unique binding sites. A four-residue glycine linker followed by a HA tag was added to the C terminus. After optimization of codon usage for chicken and removal of unwanted restriction enzyme recognition sites through synonymous nucleotide substitutions, the sequence was synthesized by GenScript Corp. Mini-nebulin was then inserted into the multicloning site of pEGFP-C2 (Takara Bio Inc.) using XhoI and SacI restriction sites, which fused GFP to the N terminus of mini-nebulin. The final mini-nebulin–GFP construct was ∼11.6 kb and resulted in a 2,543-residue protein. Mini-nebulin was also inserted into a modified pEGFP-C2 vector in which GFP was replaced with mCherry. An anti-GFP or anti–N-terminal nebulin antibody was used for analysis of mini-nebulin by immunofluorescence microscopy. Localization of the HA tag to the Z-disc was confirmed by costaining for α-actinin.

Online supplemental material

Fig. S1 shows that in control cells, GFP-actin assembles at the ends of the thin filaments, but in nebulin-depleted cells, it incorporates uniformly along the length of the thin filaments. Fig. S2 depicts a series of timed images from representative FRAP experiments. Online supplemental material is available at http://www.jcb.org/cgi/content/full/jcb.201001043/DC1.

We are grateful to Verena Koenning and Katrina Garvey for preparing the chick skeletal myocyte cultures and other technical assistance. We also thank Chinedu Nworu for cloning chicken Tmod1, Yasuko Ono for cloning chicken α-skeletal actin, Andy Warkman for the initial subcloning of mini-nebulin, Joseph Sanger (State University of New York Upstate Medical University, Syracuse, NY) and Ronald Lynch (The University of Arizona, Tucson, AZ) for advice on FRAP analysis, and the JMST graduate group (The University of Arizona) for helpful discussions.

This work was supported by National Institutes of Health (NIH) grants HL57461 and HL083146 to C.C. Gregorio, NIH grant HL093694 to P.A. Krieg, and a Nation Science Foundation Integrative Graduate Education and Research Traineeship in Genomics at the University of Arizona, an American Heart Association Predoctoral Fellowship, and an Achievement Rewards for College Scientists Foundation (Phoenix Chapter) scholarship to C.T. Pappas.

Submitted: 11 January 2010
Accepted: 28 April 2010

References

Ao, X., and S.S. Lehrer. 1995. Phalloidin unzips nebulin from thin filaments in skeletal myofibrils. *J. Cell Sci.* 108:3397–3403.

Aronson, J. 1961. Sarcomere size in developing muscles of a tarsonemid mite. *J. Biophys. Biochem. Cytol.* 11:147–156. doi:10.1083/jcb.11.1.147

Bang, M.L., R.E. Mudry, A.S. McElhinny, K. Trombitás, A.J. Geach, R. Yamasaki, H. Sorimachi, H. Granzier, C.C. Gregorio, and S. Labeit. 2001. Myopalladin, a novel 145-kilodalton sarcomeric protein with multiple roles in Z-disc and I-band protein assemblies. *J. Cell Biol.* 153:413–427. doi:10.1083/jcb.153.2.413

Bang, M.L., C. Gregorio, and S. Labeit. 2002. Molecular dissection of the interaction of desmin with the C-terminal region of nebulin. *J. Struct. Biol.* 137:119–127. doi:10.1006/jsbi.2002.4457

Bang, M.L., X. Li, R. Littlefield, S. Bremner, A. Thor, K.U. Knowlton, R.L. Lieber, and J. Chen. 2006. Nebulin-deficient mice exhibit shorter thin filament lengths and reduced contractile function in skeletal muscle. *J. Cell Biol.* 173:905–916. doi:10.1083/jcb.200603119

Bang, M.L., M. Caremani, E. Brunello, R. Littlefield, R.L. Lieber, J. Chen, V. Lombardi, and M. Linari. 2009. Nebulin plays a direct role in promoting strong actin-myosin interactions. *FASEB J.* 23:4117–4125. doi:10.1096/fj.09-137729

Bernstein, B.W., and J.R. Bamburg. 1982. Tropomyosin binding to F-actin protects the F-actin from disassembly by brain actin-depolymerizing factor (ADF). *Cell Motil.* 2:1–8. doi:10.1002/cm.970020102

Broschat, K.O. 1990. Tropomyosin prevents depolymerization of actin filaments from the pointed end. *J. Biol. Chem.* 265:21323–21329.

Caldwell, J.E., S.G. Heiss, V. Mermall, and J.A. Cooper. 1989. Effects of CapZ, an actin capping protein of muscle, on the polymerization of actin. *Biochemistry*. 28:8506–8514. doi:10.1021/bi00447a036

Castillo, A., R. Nowak, K.P. Littlefield, V.M. Fowler, and R.S. Littlefield. 2009. A nebulin ruler does not dictate thin filament lengths. *Biophys. J.* 96:1856–1865. doi:10.1016/j.bpj.2008.10.053

Chandra, M., R. Mamidi, S. Ford, C. Hidalgo, C. Witt, C. Ottenheijm, S. Labeit, and H. Granzier. 2009. Nebulin alters cross-bridge cycling kinetics and increases thin filament activation: a novel mechanism for increasing tension and reducing tension cost. *J. Biol. Chem.* 284:30889–30896. doi:10.1074/jbc.M109.049718

Chen, M.J., C.L. Shih, and K. Wang. 1993. Nebulin as an actin zipper. A two-module nebulin fragment promotes actin nucleation and stabilizes actin filaments. *J. Biol. Chem.* 268:20327–20334.

Clark, K.A., A.S. McElhinny, M.C. Beckerle, and C.C. Gregorio. 2002. Striated muscle cytoarchitecture: an intricate web of form and function. *Annu. Rev. Cell Dev. Biol.* 18:637–706. doi:10.1146/annurev.cellbio.18.012502.105840

Coluccio, L.M., and L.G. Tilney. 1984. Phalloidin enhances actin assembly by preventing monomer dissociation. *J. Cell Biol.* 99:529–535. doi:10.1083/jcb.99.2.529

Conover, G.M., S.N. Henderson, and C.C. Gregorio. 2009. A myopathy-linked desmin mutation perturbs striated muscle actin filament architecture. *Mol. Biol. Cell*. 20:834–845. doi:10.1091/mbc.E08-07-0753

Cooper, J.A. 2002. Actin dynamics: tropomyosin provides stability. *Curr. Biol.* 12:R523–R525. doi:10.1016/S0960-9822(02)01028-X

Coué, M., S.L. Brenner, I. Spector, and E.D. Korn. 1987. Inhibition of actin polymerization by latrunculin A. *FEBS Lett.* 213:316–318. doi:10.1016/0014-5793(87)81513-2

Fattoum, A., J.H. Hartwig, and T.P. Stossel. 1983. Isolation and some structural and functional properties of macrophage tropomyosin. *Biochemistry*. 22:1187–1193. doi:10.1021/bi00274a031

Gokhin, D.S., M.L. Bang, J. Zhang, J. Chen, and R.L. Lieber. 2009. Reduced thin filament length in nebulin-knockout skeletal muscle alters isometric contractile properties. *Am. J. Physiol. Cell Physiol.* 296:C1123–C1132. doi:10.1152/ajpcell.00503.2008

Goldfarb, L.G., P. Vicart, H.H. Goebel, and M.C. Dalakas. 2004. Desmin myopathy. *Brain*. 127:723–734. doi:10.1093/brain/awh033

Granger, B.L., and E. Lazarides. 1979. Desmin and vimentin coexist at the periphery of the myofibril Z disc. *Cell*. 18:1053–1063. doi:10.1016/0092-8674(79)90218-6

Gregorio, C.C., and V.M. Fowler. 1995. Mechanisms of thin filament assembly in embryonic chick cardiac myocytes: tropomodulin requires tropomyosin for assembly. *J. Cell Biol.* 129:683–695. doi:10.1083/jcb.129.3.683

Gregorio, C.C., A. Weber, M. Bondad, C.R. Pennise, and V.M. Fowler. 1995. Requirement of pointed-end capping by tropomodulin to maintain actin filament length in embryonic chick cardiac myocytes. *Nature*. 377:83–86. doi:10.1038/377083a0

Helfman, D.M., C. Berthier, J. Grossman, M. Leu, E. Ehler, E. Perriard, and J.C. Perriard. 1999. Nonmuscle tropomyosin-4 requires coexpression with other low molecular weight isoforms for binding to thin filaments in cardiomyocytes. *J. Cell Sci.* 112:371–380.

Hitchcock, S.E., L. Carisson, and U. Lindberg. 1976. Depolymerization of F-actin by deoxyribonuclease I. *Cell*. 7:531–542. doi:10.1016/0092-8674(76)90203-8

Horowits, R. 2006. Nebulin regulation of actin filament lengths: new angles. *Trends Cell Biol.* 16:121–124. doi:10.1016/j.tcb.2006.01.003

Jin, J.P., and K. Wang. 1991. Nebulin as a giant actin-binding template protein in skeletal muscle sarcomere. Interaction of actin and cloned human nebulin fragments. *FEBS Lett.* 281:93–96. doi:10.1016/0014-5793(91)80366-B

Kazmierski, S.T., P.B. Antin, C.C. Witt, N. Huebner, A.S. McElhinny, S. Labeit, and C.C. Gregorio. 2003. The complete mouse nebulin gene sequence and the identification of cardiac nebulin. *J. Mol. Biol.* 328:835–846. doi:10.1016/S0022-2836(03)00348-6

Kruger, M., J. Wright, and K. Wang. 1991. Nebulin as a length regulator of thin filaments of vertebrate skeletal muscles: correlation of thin filament length, nebulin size, and epitope profile. *J. Cell Biol.* 115:97–107. doi:10.1083/jcb.115.1.97

Labeit, S., and B. Kolmerer. 1995. The complete primary structure of human nebulin and its correlation to muscle structure. *J. Mol. Biol.* 248:308–315.

Labeit, S., T. Gibson, A. Lakey, K. Leonard, M. Zeviani, P. Knight, J. Wardale, and J. Trinick. 1991. Evidence that nebulin is a protein-ruler in muscle thin filaments. *FEBS Lett.* 282:313–316. doi:10.1016/0014-5793(91)80503-U

Lehtokari, V.L., K. Pelin, M. Sandbacka, S. Ranta, K. Donner, F. Muntoni, C. Sewry, C. Angelini, K. Bushby, P. Van den Bergh, et al. 2006. Identification of 45 novel mutations in the nebulin gene associated with autosomal recessive nemaline myopathy. *Hum. Mutat.* 27:946–956. doi:10.1002/humu.20370

Li, Z., M. Mericskay, O. Agbulut, G. Butler-Browne, L. Carlsson, L.E. Thornell, C. Babinet, and D. Paulin. 1997. Desmin is essential for the tensile strength and integrity of myofibrils but not for myogenic commitment, differentiation, and fusion of skeletal muscle. *J. Cell Biol.* 139:129–144. doi:10.1083/jcb.139.1.129

Littlefield, R., and V.M. Fowler. 1998. Defining actin filament length in striated muscle: rulers and caps or dynamic stability? *Annu. Rev. Cell Dev. Biol.* 14:487–525. doi:10.1146/annurev.cellbio.14.1.487

Littlefield, R.S., and V.M. Fowler. 2008. Thin filament length regulation in striated muscle sarcomeres: pointed-end dynamics go beyond a nebulin ruler. *Semin. Cell Dev. Biol.* 19:511–519. doi:10.1016/j.semcdb.2008.08.009

Littlefield, R., A. Almenar-Queralt, and V.M. Fowler. 2001. Actin dynamics at pointed ends regulates thin filament length in striated muscle. *Nat. Cell Biol.* 3:544–551. doi:10.1038/35078517

McElhinny, A.S., B. Kolmerer, V.M. Fowler, S. Labeit, and C.C. Gregorio. 2001. The N-terminal end of nebulin interacts with tropomodulin at the pointed ends of the thin filaments. *J. Biol. Chem.* 276:583–592. doi:10.1074/jbc.M005693200

McElhinny, A.S., S.T. Kazmierski, S. Labeit, and C.C. Gregorio. 2003. Nebulin: the nebulous, multifunctional giant of striated muscle. *Trends Cardiovasc. Med.* 13:195–201. doi:10.1016/S1050-1738(03)00076-8

McElhinny, A.S., C. Schwach, M. Valichnac, S. Mount-Patrick, and C.C. Gregorio. 2005. Nebulin regulates the assembly and lengths of the thin filaments in striated muscle. *J. Cell Biol.* 170:947–957. doi:10.1083/jcb.200502158

Milner, D.J., G. Weitzer, D. Tran, A. Bradley, and Y. Capetanaki. 1996. Disruption of muscle architecture and myocardial degeneration in mice lacking desmin. *J. Cell Biol.* 134:1255–1270. doi:10.1083/jcb.134.5.1255

Mudry, R.E., C.N. Perry, M. Richards, V.M. Fowler, and C.C. Gregorio. 2003. The interaction of tropomodulin with tropomyosin stabilizes thin filaments in cardiac myocytes. *J. Cell Biol.* 162:1057–1068. doi:10.1083/jcb.200305031

Nawrotzki, R., D.A. Fischman, and T. Mikawa. 1995. Antisense suppression of skeletal muscle myosin light chain-1 biosynthesis impairs myofibrillogenesis in cultured myotubes. *J. Muscle Res. Cell Motil.* 16:45–56. doi:10.1007/BF00125309

Nwe, T.M., K. Maruyama, and Y. Shimada. 1999. Relation of nebulin and connectin (titin) to dynamics of actin in nascent myofibrils of cultured skeletal muscle cells. *Exp. Cell Res.* 252:33–40. doi:10.1006/excr.1999.4611

Ojima, K., Z.X. Lin, M. Bang, S. Holtzer, R. Matsuda, S. Labeit, H.L. Sweeney, and H. Holtzer. 2000. Distinct families of Z-line targeting modules in the COOH-terminal region of nebulin. *J. Cell Biol.* 150:553–566. doi:10.1083/jcb.150.3.553

Ono, S., and K. Ono. 2002. Tropomyosin inhibits ADF/cofilin-dependent actin filament dynamics. *J. Cell Biol.* 156:1065–1076. doi:10.1083/jcb.200110013

Ottenheijm, C.A., C. Fong, P. Vangheluwe, F. Wuytack, G.J. Babu, M. Periasamy, C.C. Witt, S. Labeit, and H. Granzier. 2008. Sarcoplasmic reticulum calcium uptake and speed of relaxation are depressed in nebulin-free skeletal muscle. *FASEB J.* 22:2912–2919. doi:10.1096/fj.07-104372

Ottenheijm, C.A., C.C. Witt, G.J. Stienen, S. Labeit, A.H. Beggs, and H. Granzier. 2009. Thin filament length dysregulation contributes to muscle weakness in nemaline myopathy patients with nebulin deficiency. *Hum. Mol. Genet.* 18:2359–2369. doi:10.1093/hmg/ddp168

Panaviene, Z., X.A. Deng, M. Esham, and C.L. Moncman. 2007. Targeting of nebulin fragments to the cardiac sarcomere. *Exp. Cell Res.* 313:896–909. doi:10.1016/j.yexcr.2006.12.016

Pappas, C.T., N. Bhattacharya, J.A. Cooper, and C.C. Gregorio. 2008. Nebulin interacts with CapZ and regulates thin filament architecture within the Z-disc. *Mol. Biol. Cell*. 19:1837–1847. doi:10.1091/mbc.E07-07-0690

Pelin, K., P. Hilpelä, K. Donner, C. Sewry, P.A. Akkari, S.D. Wilton, D. Wattanasirichaigoon, M.L. Bang, T. Centner, F. Hanefeld, et al. 1999. Mutations in the nebulin gene associated with autosomal recessive nemaline myopathy. *Proc. Natl. Acad. Sci. USA*. 96:2305–2310. doi:10.1073/pnas.96.5.2305

Pfuhl, M., S.J. Winder, and A. Pastore. 1994. Nebulin, a helical actin binding protein. *EMBO J.* 13:1782–1789.

Root, D.D., and K. Wang. 1994. Calmodulin-sensitive interaction of human nebulin fragments with actin and myosin. *Biochemistry*. 33:12581–12591. doi:10.1021/bi00208a008

Root, D.D., and K. Wang. 2001. High-affinity actin-binding nebulin fragments influence the actoS1 complex. *Biochemistry*. 40:1171–1186. doi:10.1021/bi0015010

Sanoudou, D., and A.H. Beggs. 2001. Clinical and genetic heterogeneity in nemaline myopathy—a disease of skeletal muscle thin filaments. *Trends Mol. Med.* 7:362–368. doi:10.1016/S1471-4914(01)02089-5

Schafer, D.A., C. Hug, and J.A. Cooper. 1995. Inhibition of CapZ during myofibrillogenesis alters assembly of actin filaments. *J. Cell Biol.* 128:61–70. doi:10.1083/jcb.128.1.61

Shimizu, N., and T. Obinata. 1986. Actin concentration and monomer-polymer ratio in developing chicken skeletal muscle. *J. Biochem.* 99:751–759.

Sussman, M.A., S. Baqué, C.S. Uhm, M.P. Daniels, R.L. Price, D. Simpson, L. Terracio, and L. Kedes. 1998. Altered expression of tropomodulin in cardiomyocytes disrupts the sarcomeric structure of myofibrils. *Circ. Res.* 82:94–105.

Tonino, P., C.T. Pappas, B.D. Hudson, S. Labeit, C.C. Gregorio, and H. Granzier. 2010. Reduced myofibrillar connectivity and increased Z-disk width in nebulin-deficient skeletal muscle. *J. Cell Sci.* 123:384–391. doi:10.1242/jcs.042234

Trinick, J. 1994. Titin and nebulin: protein rulers in muscle? *Trends Biochem. Sci.* 19:405–409. doi:10.1016/0968-0004(94)90088-4

Wang, J., J.M. Sanger, and J.W. Sanger. 2005a. Differential effects of Latrunculin-A on myofibrils in cultures of skeletal muscle cells: insights into mechanisms of myofibrillogenesis. *Cell Motil. Cytoskeleton*. 62:35–47. doi:10.1002/cm.20083

Wang, J., N. Shaner, B. Mittal, Q. Zhou, J. Chen, J.M. Sanger, and J.W. Sanger. 2005b. Dynamics of Z-band based proteins in developing skeletal muscle cells. *Cell Motil. Cytoskeleton*. 61:34–48. doi:10.1002/cm.20063

Wang, J., J.M. Sanger, S. Kang, H. Thurston, L.Z. Abbott, D.K. Dube, and J.W. Sanger. 2007. Ectopic expression and dynamics of TPM1alpha and TPM1kappa in myofibrils of avian myotubes. *Cell Motil. Cytoskeleton*. 64:767–776. doi:10.1002/cm.20221

Wang, J., H. Thurston, E. Essandoh, M. Otoo, M. Han, A. Rajan, S. Dube, R.W. Zajdel, J.M. Sanger, K.K. Linask, et al. 2008. Tropomyosin expression and dynamics in developing avian embryonic muscles. *Cell Motil. Cytoskeleton*. 65:379–392. doi:10.1002/cm.20267

Wang, K., M. Knipfer, Q.Q. Huang, A. van Heerden, L.C. Hsu, G. Gutierrez, X.L. Quian, and H. Stedman. 1996. Human skeletal muscle nebulin sequence encodes a blueprint for thin filament architecture. Sequence motifs and affinity profiles of tandem repeats and terminal SH3. *J. Biol. Chem.* 271:4304–4314. doi:10.1074/jbc.271.8.4304

Weber, A., C.R. Pennise, G.G. Babcock, and V.M. Fowler. 1994. Tropomodulin caps the pointed ends of actin filaments. *J. Cell Biol.* 127:1627–1635. doi:10.1083/jcb.127.6.1627

Weber, A., C.R. Pennise, and V.M. Fowler. 1999. Tropomodulin increases the critical concentration of barbed end-capped actin filaments by converting ADP.P(i)-actin to ADP-actin at all pointed filament ends. *J. Biol. Chem.* 274:34637–34645. doi:10.1074/jbc.274.49.34637

Witt, C.C., C. Burkart, D. Labeit, M. McNabb, Y. Wu, H. Granzier, and S. Labeit. 2006. Nebulin regulates thin filament length, contractility, and Z-disk structure in vivo. *EMBO J.* 25:3843–3855. doi:10.1038/sj.emboj.7601242

Wright, J., Q.Q. Huang, and K. Wang. 1993. Nebulin is a full-length template of actin filaments in the skeletal muscle sarcomere: an immunoelectron microscopic study of its orientation and span with site-specific monoclonal antibodies. *J. Muscle Res. Cell Motil.* 14:476–483. doi:10.1007/BF00297210

Zhukarev, V., J.M. Sanger, J.W. Sanger, Y.E. Goldman, and H. Shuman. 1997. Distribution and orientation of rhodamine-phalloidin bound to thin filaments in skeletal and cardiac myofibrils. *Cell Motil. Cytoskeleton*. 37:363–377. doi:10.1002/(SICI)1097-0169(1997)37:4<363::AID-CM7>3.0.CO;2-5